Redox Biology 19 (2018) 81–91

Contents lists available at ScienceDirect

Redox Biology

journal homepage: www.elsevier.com/locate/redox

Folic acid modulates *VPO1* DNA methylation levels and alleviates oxidative stress-induced apoptosis in vivo and in vitro

Shanshan Cui[a,1], Xin Lv[a,1], Wen Li[a], Zhenshu Li[a], Huan Liu[a], Yuxia Gao[b,*], Guowei Huang[a,*]

[a] Department of Nutrition and Food Science, School of Public Health, Tianjin Medical University, 22 Qixiangtai Road, Heping District, Tianjin 300070, China
[b] Department of Cardiology, General Hospital of Tianjin Medical University, Tianjin 300052, China

ARTICLE INFO

Keywords:
Folic acid
DNA methylation
Vascular peroxidase 1
Apoptosis
Oxidative stress
Atherosclerosis

ABSTRACT

Endothelial cell injury and apoptosis play a primary role in the pathogenesis of atherosclerosis. Moreover, accumulating evidence indicates that oxidative injury is an important risk factor for endothelial cell damage. In addition, low folate levels are considered a contributing factor to promotion of vascular disease because of the deregulation of DNA methylation. We aimed to investigate the effects of folic acid on injuries induced by oxidative stress that occur via an epigenetic gene silencing mechanism in ApoE knockout mice fed a high-fat diet and in human umbilical vein endothelial cells treated with oxidized low-density lipoprotein (ox-LDL). We assessed how folic acid influenced the levels of 8-hydroxy-2′-deoxyguanosine (8-OHdG, an oxidative DNA damage marker) and cellular apoptosis in in vivo and in vitro models. Furthermore, we analyzed DNA methyltransferase (DNMT) activity, vascular peroxidase 1 (VPO1) expression, and promoter methylation in human umbilical vein endothelial cells. Our data showed that folic acid reduced 8-OHdG levels and decreased apoptosis in the aortic tissue of ApoE$^{-/-}$ mice. Likewise, our in vitro experiments showed that folic acid protects against endothelial dysfunction induced by ox-LDL by reducing reactive oxygen species (ROS)-derived oxidative injuries, 8-OHdG content, and the apoptosis ratio. Importantly, this effect was indirectly caused by increased DNMT activity and altered DNA methylation at *VPO1* promoters, as well as changes in the abundance of VPO1 expression. Collectively, we conclude that folic acid supplementation may prevent oxidative stress-induced apoptosis and suppresses ROS levels through downregulating VPO1 as a consequence of changes in DNA methylation, which may contribute to beneficial effects on endothelial function.

1. Introduction

Cardiovascular diseases (CVDs) represent a major public health problem worldwide considering their high morbidity and disease burden. Among these, atherosclerotic cardiovascular disease remains a leading cause of death and disability [1,2]. It has been confirmed that endothelial cell injury and apoptosis play primary roles in the pathogenesis of atherosclerosis (AS) [3,4], and accumulating evidence indicates that oxidative injury represents an important risk factor for endothelial cell damage [5,6]. The subendothelial retention of low-density lipoprotein (LDL) and its oxidative modification, oxidized LDL (ox-LDL), activates signaling pathways resulting in an oxidative stress response, which eventually leads to AS [7,8]. Vascular peroxidase 1 (VPO1), a recently identified member of the peroxidase family in the cardiovascular system [9], contributes to oxidation and retention of LDL in vessel walls [10]. As a result, VPO1 may represent a novel mediator of AS. Therefore, uncovering the molecular mechanisms underlying oxidative stress-induced endothelial cell damage is of utmost clinical importance for the prevention and treatment of AS.

Recent findings suggest that the pathogenesis of AS involves dynamic changes in epigenetic markers and gene expression [11,12]. Furthermore, human studies have noted differentially methylated

Abbreviations: 5-mC, 5-methylcytosine; 8-OHdG, 8-hydroxy-2′-deoxyguanosine; AS, atherosclerosis; CAT, catalase; CpGs, cytosine-phosphate-guanines; CVD, cardiovascular disease; DNMT, DNA methyltransferase; FITC, fluorescein isothiocyanate; Gpx, glutathione peroxidase; HFD, high-fat diet; HUVECs, human umbilical vein endothelial cells; LDH, lactate dehydrogenase; MALDI-TOF, matrix-assisted laser desorption/ionization time-of-flight; MDA, malondialdehyde; MTS, 3-(4,5-dimethylthiazol-2-yl)-5-(3-carboxymethoxyphenyl)-2-(4-sulfophenyl)-2H-tetrazolium; ox-LDL, oxidized low-density lipoprotein; PCR, polymerase chain reaction; ROS, reactive oxygen species; SAH, S-adenosylhomocysteine; SAM, S-adenosylmethionine; SOD, superoxide dismutase; T-AOC, total antioxidant capacity; VPO1, vascular peroxidase 1; WT, wild-type

* Corresponding authors.
E-mail addresses: gaoyuxiatj@tmu.edu.cn (Y. Gao), huangguowei@tmu.edu.cn (G. Huang).
[1] The two authors contributed equally to the paper, so they are both first authors.

https://doi.org/10.1016/j.redox.2018.08.005
Received 13 June 2018; Received in revised form 2 August 2018; Accepted 7 August 2018
Available online 08 August 2018

cytosine-phosphate-guanines (CpGs) as an accompanying feature of AS [13–15]. DNA methylation is generally catalyzed by DNA methyltransferases (DNMTs), and methyl groups are added to the C5 position of cytosine residues; this is typically associated with transcriptional repression [16,17]. Importantly, epigenetic regulation is not static, as it can be altered by environmental stimuli such as nutrition and dietary supplements [18,19]. These findings imply a potential role for DNA methylation in AS. However, the epigenetic mechanisms remain to be further clarified.

Folic acid, an oxidized form of folate with high bioavailability, is the major component of one-carbon metabolism, including nucleotide metabolism, maintaining the cellular redox status and methylation metabolism [20]. Folate inadequacy has been linked to endothelial dysfunction and CVDs via epigenetic changes [21,22]. Epidemiological studies [23,24] have shown a decline in cardiovascular risk within countries with folic acid-fortified foods. The beneficial effect of folic acid is partially attributed to the epigenetic mechanisms in which folic acid acts as a methyl group donor. Moreover, a recent study has reported that folic acid is a micronutrient that can function as a novel redox regulator [25]. We also recently showed that folic acid alleviates atherogenesis by reducing plasma homocysteine levels and improving the antioxidant capacity in rats fed a high-fat diet (HFD) [26]; however, the mechanism underlying the relationship between folic acid and endothelial cell injury remains unclear.

Our previous study [27] has demonstrated that folic acid supplementation effectively prevents AS by regulating the normal homocysteine state, upregulating the S-adenosylmethionine (SAM): S-adenosylhomocysteine (SAH) ratio, and elevating DNMT activity. These results support that an increase in folic acid levels triggers epigenetic mechanisms to ameliorate AS. In the present study, we expanded our previous work to investigate the mechanism underlying the effects of folic acid on endothelial cell injury and apoptosis, employing ApoE knockout ($ApoE^{-/-}$) mice and human umbilical vein endothelial cells (HUVECs). Additionally, the primary goals of this study were to identify the epigenetic regulatory mechanisms underlying the folic acid-induced inhibition of VPO1 expression and to determine the redox signaling pathway by which folic acid attenuates endothelial cell injury.

2. Material and methods

2.1. Animals, diets, and experimental procedures

A total of 24 homozygous $ApoE^{-/-}$ mice from a C57BL/6 J background (male, 4 weeks old) and 8 age-matched male C57BL/6 J mice were purchased from Peking Huafukang Laboratory Animal Center (Beijing, China). $ApoE^{-/-}$ mice were randomly distributed into three groups (8 per group): (1) high-fat plus folic acid-deficient diet (HF + DEF), (2) HFD plus control diet (HF + CON), and (3) HFD plus daily intragastric gavage with 60 μg/kg body weight folic acid (HF + FA). In addition, 8 C57BL/6 J mice were used as wild-type (WT) controls. The folate-deficient diet (containing 0.2 mg folic acid/kg diet) and control diet (2.1 mg folic acid/kg diet) were purchased from TestDiet (St. Louis, MO, USA). All mice were fed a Western-type HFD [28] (21% fat, 1.25% cholesterol) and subjected to intragastric administration (folic acid or isometric 0.9% saline) for 20 weeks, when the mice reached the age of 24 weeks. The calculated nutritional composition of the HFD diet is listed in Supplementary Table 1. The mice were group housed in a temperature-controlled room (22.5 ± 0.5 °C) with a 12:12/h light/dark cycle and provided food and water ad libitum over the 20-week experimental period. The study was approved by the ethics committee of the Tianjin Medical University (TMUaMEC 2015009).

After 20 weeks, all mice were fasted overnight and then sacrificed via suffocation with CO_2. Blood was collected by cardiac puncture with a syringe and centrifuged for the preparation of plasma and serum. The plasma, serum, and aorta were immediately collected and stored at −80 °C until analysis.

2.2. HUVEC culture

HUVECs were obtained from GuangZhou Jennio Biotech Co., Ltd (Guangzhou, China) and were cultured in M199 medium (Yuanpei Biotechnology Co., Ltd, Shanghai, China) with 10% (v/v) fetal bovine serum (Gibco BRL, Grand Island, NY, USA), 100 IU/mL penicillin G, and 100 IU/mL streptomycin. The cells were incubated at 37 °C in a humidified atmosphere of 5% CO_2 and used at passages 3–5. HUVECs were exposed to the indicated concentrations of folic acid (0–1000 nmol/L) for 48 h and exposed to medium containing 120 μg/mL of ox-LDL or control vehicle for the first 24 h.

2.3. Immunofluorescence staining

Aortic arch samples fixed in 4% paraformaldehyde, embedded in paraffin, and sectioned into consecutive 8-μm thick free-floating sections were de-waxed, hydrated, and then repaired using sodium citrate-EDTA. Sections were blocked with goat serum for 1 h at 37 °C and then reacted with mouse anti-8-hydroxy-2'-deoxyguanosine (8-OHdG) antibody (1:500; StressMarq Biosciences, Victoria, BC, Canada) at 4 °C overnight. The sections were washed with PBS and reacted with fluorescein isothiocyanate (FITC) -conjugated goat anti-mouse secondary antibodies (1:100) for 1 h at 25 °C. Antifade mounting medium with DAPI (Vector Laboratories, Burlingame, CA, USA) was used to dye the nuclei and for mounting. Images were obtained using a fluorescence microscope (Olympus, Tokyo, Japan). Positive cells were counted using Image Pro Plus 6.0 software.

2.4. TUNEL assay

Sections of the aortic arch were assayed with the Apoptosis Detection Kit (Roche, Basel, Switzerland). Sections were de-waxed, hydrated, blocked with Proteinase K solution for 20 min at 37 °C, and then reacted with TUNEL solution for 30 min at 37 °C in the dark. The sections were washed with PBS, reacted with Converter POD solution for 30 min at 37 °C in the dark, and visualized using a DBA Elite kit (Dingguo Changsheng Biotechnology Co., Ltd, Beijing, China). The images were obtained using microscopy (Olympus), and positive cells were counted using Image Pro Plus 6.0 software.

2.5. Measurement of plasma ox-LDL concentration

The plasma ox-LDL concentration was detected using the mouse ox-LDL ELISA Kit (CUSABIO TECHNOLOGY, Wuhan, China) according to the manufacturer's instructions. This assay employs the quantitative sandwich enzyme immunoassay technique. Antibodies specific for ox-LDL were precoated onto a microplate. Then, the absorbance at 490 nm was recorded using a microplate reader (ELX800uv™; BioTek Instruments Inc, Winooski, VT, USA) within 5 min. Data were analyzed using the Curve Expert 1.3 software (CUSABIO TECHNOLOGY) to generate the standard curve.

2.6. DNMT activity assay

HUVEC nuclear extracts were isolated using the nuclear extraction kit (Merck, Darmstadt, Germany). DNMT activity was measured using a colorimetric DNMT activity/inhibition assay kit (Epigentek Group Inc., Farmingdale, NY, USA) according to the manufacturer's instructions. This sensitive ELISA-based method uses the ability of proteins containing methyl CpG-binding domains to bind methylated DNA with high affinity. The cellular protein content was determined using a BCA protein assay kit (BosterBio, Wuhan, China). Optical density (OD) was measured on a microplate reader at 450 nm, and DNMT activity [(OD)/

(h·mg)] was calculated according to the following formula:

$$\text{DNMT activity (OD/h/mg)} = \frac{average\ sample\ OD - average\ blank\ OD}{protein\ amount\ (\mu g)^{*} \times hour^{**}} \times 1000$$

where * indicates the protein amount added into the reaction, and ** indicates the incubation time.

2.7. Global DNA methylation assay

Total cellular DNA was isolated using a genomic DNA purification kit (Promega Corporation, Beijing, China). Global methylation levels were measured using a Global DNA Methylation (5-mC) colorimetric ELISA Easy Kit (Epigentek Group Inc). According to the manufacturer's instructions, DNA was immobilized on the strip well, which is specifically coated with a DNA affinity substance. The methylated DNA fraction can then be recognized by a 5-methylcytosine antibody and quantified via an ELISA-like reaction. The amount of methylated DNA is proportional to the absorbance at 450 nm.

2.8. Real-time polymerase chain reaction (PCR) analysis

Gene expression was quantified by real-time reverse transcription (RT)-PCR. Total RNA was isolated using the Eastep® Super Total RNA Extraction Kit (Promega Corporation). First-strand cDNA was synthesized from 1 μg of total RNA with the All-in-One™ First-Strand cDNA Synthesis Kit (GeneCopoeia Inc., Rockville, MD, USA) according to the standard protocol. Quantitative PCR was performed using the Roche LightCycler 480 sequence detector (Roche, Mannheim, Germany). The cDNA was amplified using a 20 μL PCR mixture containing LightCycler 480 SYBR Green I Master Mix (Roche), cDNA, and forward and reverse primers (Table 1). The reaction included an initial denaturation at 95 °C for 5 min, followed by 45 amplification cycles (denaturation, 95 °C for 10 s; annealing, 60 °C for 10 s, extension, 72 °C for 10 s). The specificity of each primer pair was confirmed using a melting curve analysis. Each sample was analyzed in duplicate, and quantification was performed with the efficiency-corrected $2^{-\Delta CT}$ method using housekeeping genes for internal normalization.

2.9. Western blotting

Western blotting was used to analyze protein expression in the cytosol of HUVEC cells. HUVECs were lysed with the cell lysis buffer (Beyotime Institute of Biotechnology, Haimen, China) and protein levels were quantified using the BCA protein assay kit (Beyotime Institute of Biotechnology), using bovine serum albumin as a standard. The extracted cellular proteins were boiled in loading buffer, and equal protein amounts were separated by 8–16% SDS-PAGE (GenScript ExpressPlus™, Piscataway, NJ, USA) and transferred to PVDF membranes (Merck Millipore Corporation, Bedford, MA, USA). Subsequently, the membranes were blocked with 5% (w/v) milk in Tris-buffered saline and 0.1% Tween 20 for 2 h at room temperature, followed by incubation with rabbit polyclonal anti-VPO1 (1:500; Merck Millipore Corporation), mouse anti-DNMT1 (1:500; Abcam, Cambridge, UK), rabbit polyclonal anti-DNMT3a (1:1000; Abcam), rabbit polyclonal anti-DNMT3b (1:500; Abcam), and rabbit polyclonal anti-β-actin antibodies (1:1000; Cell Signaling Technology, Danvers, MA, USA) overnight at 4 °C on a rocking table and washing with PBST. The membranes were then incubated with HRP-conjugated secondary antibodies diluted (1:2000; Cell Signaling Technology) for 1 h at 25 °C. Finally, the protein bands were visualized by chemiluminescence using the ECL reagent and photographed using a Bio-Spectrum Gel Imaging System (Bio-Rad, Hercules, CA, USA). A semiquantitative analysis of specific immunolabeled bands was performed by densitometric analysis using Image Pro Plus 6.0 software. The intensity of each protein band was normalized to that of the respective β-actin band.

Table 1
Nucleotide sequences of the forward and reverse primers for RT-PCR.

Gene name	Primers
VPO1	Forward: AGCCAGCCATCACCTGGAAC Reverse: TTCCGGGCCACACACTCATA
DNMT1	Forward: CGGCCTCATCGAGAAGAATATC Reverse: TGCCATTAACACCACCTTCA
DNMT3A	Forward: AGTCCGATGGAGAGGCTAAG Reverse: GTTTGGCAGGGCCCTTTG
DNMT3B	Forward: GTTTGGCAGGGCCCTTTG Reverse: ATCTTTCCCCACACGAGG
GAPDH	Forward: CCACTCCTCCACCTTTGAC Reverse: ACCCTGTTGCTGTAGCCA

2.10. VPO1 promoter methylation analysis

Quantitative methylation analysis of CpG sites in the *VPO1* promoter region was performed using the Sequenom MassARRAY platform (CapitalBio, Beijing, China). This system uses RNase-specific enzyme digestion in combination with matrix-assisted laser desorption/ionization time-of-flight (MALDI-TOF) mass spectrometry. Genomic DNA was extracted from HUVECs using the QIAamp DNA Mini Kit (Qiagen, Dusseldorf, Germany) according to the manufacturer's instructions. A total of 1.5 μg of DNA was bisulfite-treated with the EZ DNA Methylation-Gold Kit (Zymo Research, Irvine, CA, USA) according to the manufacturer's instructions. PCR primers were designed using Epidesigner (http://www.epidesigner.com). For each reverse primer, an additional T7 promoter tag for in vivo transcription was added, as well as a 10-mer tag on the forward primer to adjust for melting temperature differences. We used the following primers based on the reverse complementary strands of *VPO1*: 5′-aggaagagagGGAGGAGAGTA TTGGTATTTTTGATT-3′ and 3′-cagtaatacgactcactatagggagaaggctAAAC TCCACACAAAACCTTTCATT-5′. PCR products were purified and digested using the MassCLEAVE Kit (Sequenom). Mass spectra were obtained via Spectro CHIP® Arrays and Clean Resin Kit (Sequenom) and MassARRAY Compact MALDI-TOF (Sequenom). The methylation ratios were generated and analyzed using the EpiTYPER software (Sequenom).

2.11. Measurement of plasma and intracellular antioxidant capacity and lipid peroxidation

2.11.1. Lipid peroxidation analysis

Lipid peroxidation was evaluated in both plasma and HUVEC samples. Plasma samples and the intracellular malondialdehyde (MDA) content was assayed using commercial kits (Nanjing Jiancheng Bioengineering Institute, Nanjing, China) according the manufacturer's instructions. MDA and thiobarbituric acid react to form a Schiff base adduct under high-temperature or acidic conditions and produce a red-colored chromogenic product that can be easily measured spectrophotometrically. Cellular MDA concentrations were normalized to the cellular protein levels, determined using a BCA protein assay kit (BosterBio).

2.11.2. Determination of tissue damage markers

The content of lactate dehydrogenase (LDH) in the culture medium was assayed using commercial kits (Nanjing Jiancheng Bioengineering Institute) according to the manufacturer's instructions. LDH is a stable protein that exists in the cytoplasm of normal cells. Once the cell membrane is damaged, LDH is released into the medium. Cellular damage can be judged by detecting the LDH activity in culture medium.

2.11.3. Determination of enzymatic antioxidant activities

The intracellular total antioxidant capacity (T-AOC), glutathione peroxidase (Gpx), catalase (CAT), and plasma and intracellular superoxide dismutase (SOD) activities were assayed with commercial kits

(Nanjing Jiancheng Bioengineering Institute) according to the manufacturer's protocol. Cellular T-AOC, Gpx, CAT, and SOD activities were normalized to the cellular protein content, as determined by a BCA protein assay kit (BosterBio).

2.11.4. Measurement of intracellular reactive oxygen species (ROS) by flow cytometry

The effects of folic acid on the intracellular ROS levels in HUVECs were detected by flow cytometry using a DCFH-DA probe (Sigma-Aldrich, St. Louis, MO, USA). HUVECs were cultured and treated as described in "HUVEC culture". Cells were incubated with 10 μM DCFH-DA for 30 min in the dark, in a humidified 5% CO_2 atmosphere. The cells were washed thrice with PBS to remove the extracellular DCFH-DA fluorescence probes, collected by centrifugation, and then suspended in PBS. The fluorescence intensity was quantified by a flow cytometer (FlowSight, Merck Millipore) equipped with a 488-nm argon laser using a band pass filter of 530 nm. The mean fluorescence intensity was acquired, analyzed, and plotted using the IDEAS software (FlowSight, Merck Millipore). Data are reported as DCF fluorescence, which indicates the percentage of control cells.

2.11.5. Measurement of intracellular 8-OHdG

The levels of intracellular 8-OHdG were determined using a DNA Damage (8-OHdG) ELISA Kit (StressMarq Biosciences). The ELISA utilizes an 8-hydroxy-2-deoxy guanosine-coated plate and an HRP-conjugated antibody for detection. HUVECs were cultured and treated as described in "HUVEC culture". Total cellular DNA was isolated using the Genomic DNA Purification Kit (Promega Corporation) following the manufacturer's protocol. Then, DNA was digested with DNA digest mix (Sigma-Aldrich) for 6 h at 37 °C. 8-OHdG was measured using a competitive enzyme immune assay following the manufacturer's instructions. The absorbance at 450 nm was recorded using a microplate reader (ELX800uv™; BioTek Instruments Inc). Data were analyzed with the data analysis tool (StressMarq Biosciences).

2.11.6. Measurement of intracellular apoptosis by flow cytometry

A FITC–annexin V apoptosis detection kit (BD Pharmingen, Franklin Lakes, NJ, USA) was used to measure apoptosis by flow cytometry, according to the manufacturer's protocol. HUVECs were cultured and treated as described in "HUVEC culture". Briefly, 1×10^6 cells were collected, washed with ice-cold PBS, and double-stained with 5 μL of FITC–nnexin V and 5 μL of propidium iodide for 20 min at 25 °C in the dark. The fluorescence intensity was quantified using a flow cytometer (FlowSight, Merck Millipore) equipped with a 488 nm argon laser using a band pass filter of 530 nm. Data were acquired, analyzed, and plotted using the IDEAS software (FlowSight, Merck Millipore).

2.11.7. Cell viability assay

Cell viability was measured using the CellTiter 96® AQ_{ueous} One Solution Cell Proliferation Assay (Promega Corporation, Madison, WI, USA), which is a colorimetric method for determining the number of viable proliferating cells that can be used in cytotoxicity assays. The 3-(4,5-dimethylthiazol-2-yl)-5-(3-carboxymethoxyphenyl)-2-(4-sulfophenyl)-2H-tetrazolium (MTS) substrate is bio-reduced by living cells into a colored formazan product that is soluble in tissue culture medium. Briefly, HUVECs were cultured and treated as described in "HUVEC culture" and then seeded into a 96-well plate at a density of 1×10^4 cells per well. Next, 20 μL of CellTiter 96® AQ_{ueous} One Solution Reagent was pipetted into each well of a 96-well assay plate containing the samples in 100 μL of culture medium. The plate was incubated at 37 °C for 4 h in a humidified, 5% CO_2 atmosphere. The absorbance at 490 nm was recorded using a microplate reader (ELX800uv™; BioTek Instruments Inc).

2.11.8. Statistical analysis

Data from in vivo experiments were expressed as the means ± SD, while the data of in vitro experiments were expressed as the means ± SE. One-way analysis of variance (ANOVA) was used to evaluate differences between treatment groups, followed by least significant difference multiple comparisons to determine significant differences among the experimental groups. Student's one-tailed *t*-tests were performed to evaluate the significance of any differences between the MALDI-TOF mass spectrometry data and the data from bisulfite sequencing between test groups. For all analyses, a p-value < 0.05 was considered statistically significant. The statistical analysis was performed using SPSS, version 17.0 (IBM Corp, Chicago, IL, USA).

3. Results

3.1. Folic acid attenuates oxidative injury and apoptosis in ApoE$^{-/-}$ mice

We have recently reported that folic acid supplementation delays atherosclerotic lesion development in ApoE$^{-/-}$ mice fed HFD [27]. In addition, oxidative stress plays an important role in the pathogenesis of AS [29]. To determine whether folic acid attenuates oxidative injury, we first assessed the concentration of plasma ox-LDL and MDA (which represent an important risk factor and a biomarker of oxidative injury, respectively) and the levels of plasma antioxidant enzymes in AS model mice (Fig. 1A). After 20 weeks of treatment, ApoE$^{-/-}$ mice showed an almost 1.2-fold and 1.5-fold increase in plasma ox-LDL and MDA levels, respectively, compared with WT mice, whereas the plasma SOD activity was reduced by approximately 53%. Folic acid deficiency decreased the activity of the plasmatic antioxidant SOD ($p < 0.05$, compared with that in the HF + CON group). In contrast, folic acid supplementation significantly reduced plasma ox-LDL and MDA levels and increased SOD activity ($p < 0.05$, compared with that in the HF + DEF group).

After evaluating plasma lipid peroxidation and the levels of antioxidant enzymes, we assessed the 8-OHdG level in aortic tissues to confirm the effect of folic acid on oxidative stress in the aorta (Fig. 1B-C). 8-OHdG is a sensitive marker of oxidative DNA damage. Immunofluorescence staining of 8-OHdG showed that the positive staining ratio was significantly higher in ApoE$^{-/-}$ mice compared with that in the WT group. Furthermore, 8-OHdG staining was significantly attenuated by folic acid supplementation ($p < 0.05$, compared with the HF + CON group).

TUNEL assay was used to test the accumulation of DNA breaks, which indicate an apoptotic process, to ascertain the effect of folic acid on apoptosis in the aorta in AS model mice (Fig. 1D-E). The TUNEL-positive fraction in aortic cross-sections increased significantly in ApoE$^{-/-}$ mice ($p < 0.05$, compared with that in the WT group). Following 20 weeks of folic acid administration, the apoptotic ratio was significantly lower than that in the HF + CON and HF + DEF groups (44.55 ± 4.40% versus 57.53 ± 4.31% and 66.53 ± 7.81%, respectively).

3.2. Folic acid decreases apoptosis and increases cell viability in vitro

To investigate the cytoprotective effect of folic acid, we assessed the apoptosis rate and cell viability using flow cytometry and the MTS assay, respectively. Ox-LDL significantly reduced cell survival and increased the rate of apoptosis in HUVECs when compared with that in cells incubated without ox-LDL ($p < 0.05$, Fig. 2). Then, we determined whether folic acid protects cells from ox-LDL-induced injuries. Indeed, cell viability increased in a concentration-dependent manner with increasing folic acid concentrations. Higher folic acid concentrations (500 and 1000 nmol/L) significantly increased cell viability compared with that in the ox-LDL + FA20 group ($p < 0.05$). Consistent with in vivo data, flow cytometry results also showed that folic acid decreased apoptosis in HUVECs in a dose-dependent manner (Fig. 2C). Specifically, the apoptosis rate decreased from 9.07 ± 2.23% in the ox-LDL + FA20 group to 1.31 ± 0.15% in the ox-LDL + FA1000 group ($p < 0.05$). Similarly, microscopic images showed that cells incubated with 20 nmol/L folic acid without ox-LDL displayed normal

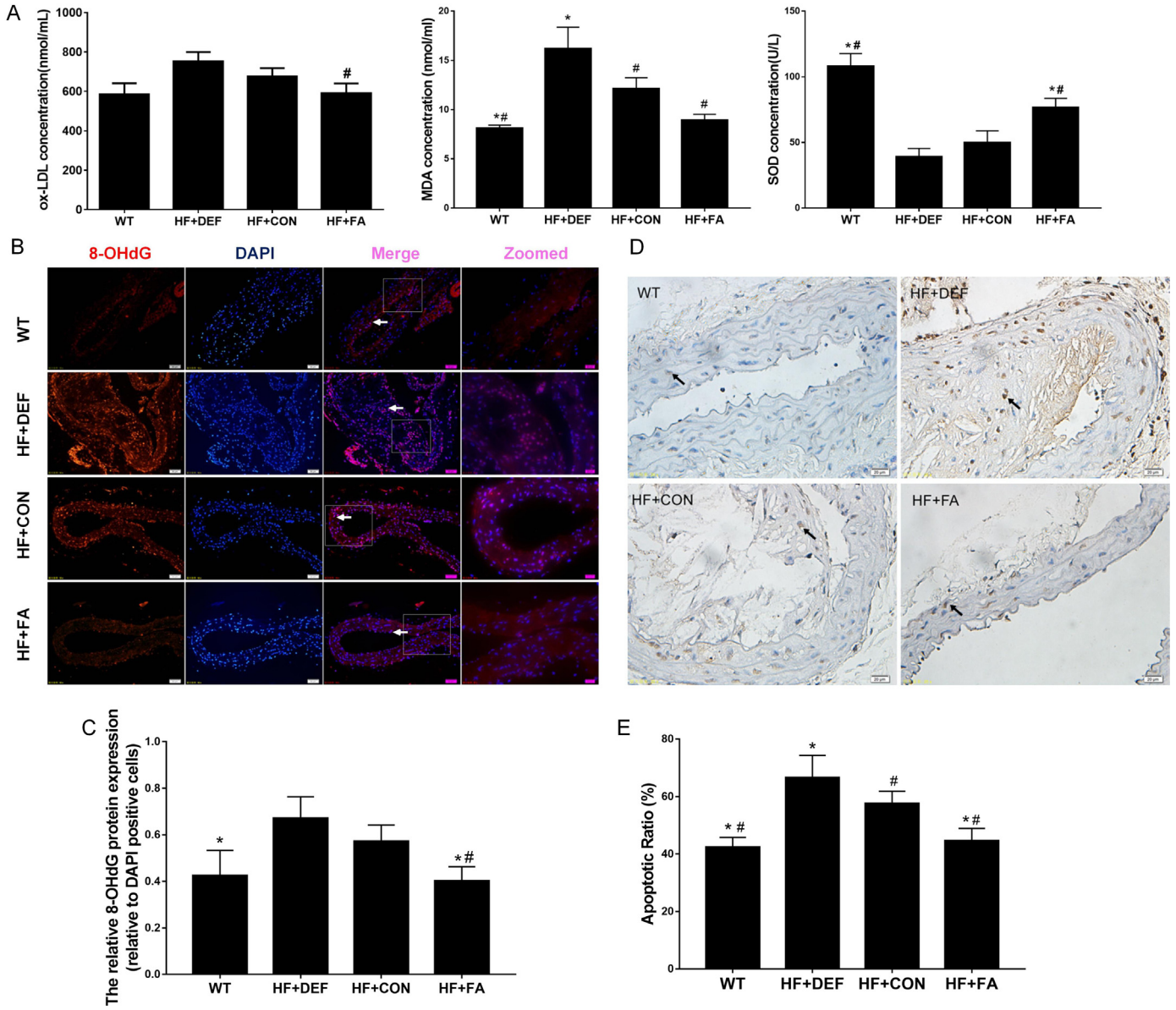

Fig. 1. Folic acid attenuates oxidative injury and cell apoptosis in ApoE$^{-/-}$ mice. Mice treated with WT, HF + DEF, HF + CON and HF + FA diet during the 20 experimental weeks. (A) Plasma oxidized low-density lipoprotein (ox-LDL) contents, malondialdehyde (MDA) contents, and superoxide dismutase (SOD) activities in mice. (B) Representative images of aortic cross-sections immunostained with markers of 8-OHdG (magnification ×200, ×400). Cell nuclei were stained with DAPI (blue). Double staining for 8-OHdG (red) and DAPI (blue) were indicated with arrows. (C) Quantitative assessment of 8-OHdG positive cells in aortic (values are mean ± SD). (D) Representative images of aortic cross-sections immunostained with markers of apoptosis (arrows); cell nuclei were stained with Mayer's hemalum solution (blue) (magnification ×400). (E) Summary of apoptosis ratio shows mean ± SD. (n = 5 mice/group) *, $p < 0.05$ compared with the HF + CON group. #, $p < 0.05$ compared with the HF + DEF group. (For interpretation of the references to color in this figure legend, the reader is referred to the web version of this article).

growth and a uniform size. Conversely, in cells incubated with ox-LDL, the shape of the cells changed dramatically as they became narrower, and a large quantity of cell debris was observed. Moreover, cellular morphology in the folate-deficient group (ox-LDL + FA0) was significantly impaired. Nevertheless, by increasing the dose of folic acid, the cellular morphology gradually recovered; specifically, after treatment with 1000 nmol/L folic acid, most cells had regained their shape.

3.3. Folic acid inhibits ox-LDL-induced endothelial cell oxidative injury

To evaluate the anti-oxidative effects of folic acid in ox-LDL-injured HUVECs, we investigated the intracellular ROS levels by flow cytometry. As shown in Fig. 3A-C, ox-LDL-treated HUVECs showed markedly higher intracellular ROS levels compared with those in the WT control group ($p < 0.05$). Moreover, folic acid treatment counteracted the ox-LDL-induced intracellular ROS production. The ROS levels generated in the ox-LDL + FA1000 group were nearly 17% lower than those in the ox-LDL + FA20 group, as reflected by the DCF fluorescence intensity.

One of the major consequences of endothelial injury involves oxidative stress-induced DNA damage; hence, we assessed the intracellular 8-OHdG levels by ELISA. We found that the level of intracellular 8-OHdG was significantly increased in ox-LDL-treated HUVECs compared with that in the WT control group ($p < 0.05$, Fig. 3D). In agreement with our ROS data, folic acid decreased the levels of intracellular 8-OHdG in a dose-dependent manner. In particular, the lowest 8-OHdG level was achieved with 1000 nmol/L folic acid (1.24 ± 0.21 ng/mL, $p < 0.05$ versus the ox-LDL + FA20 group).

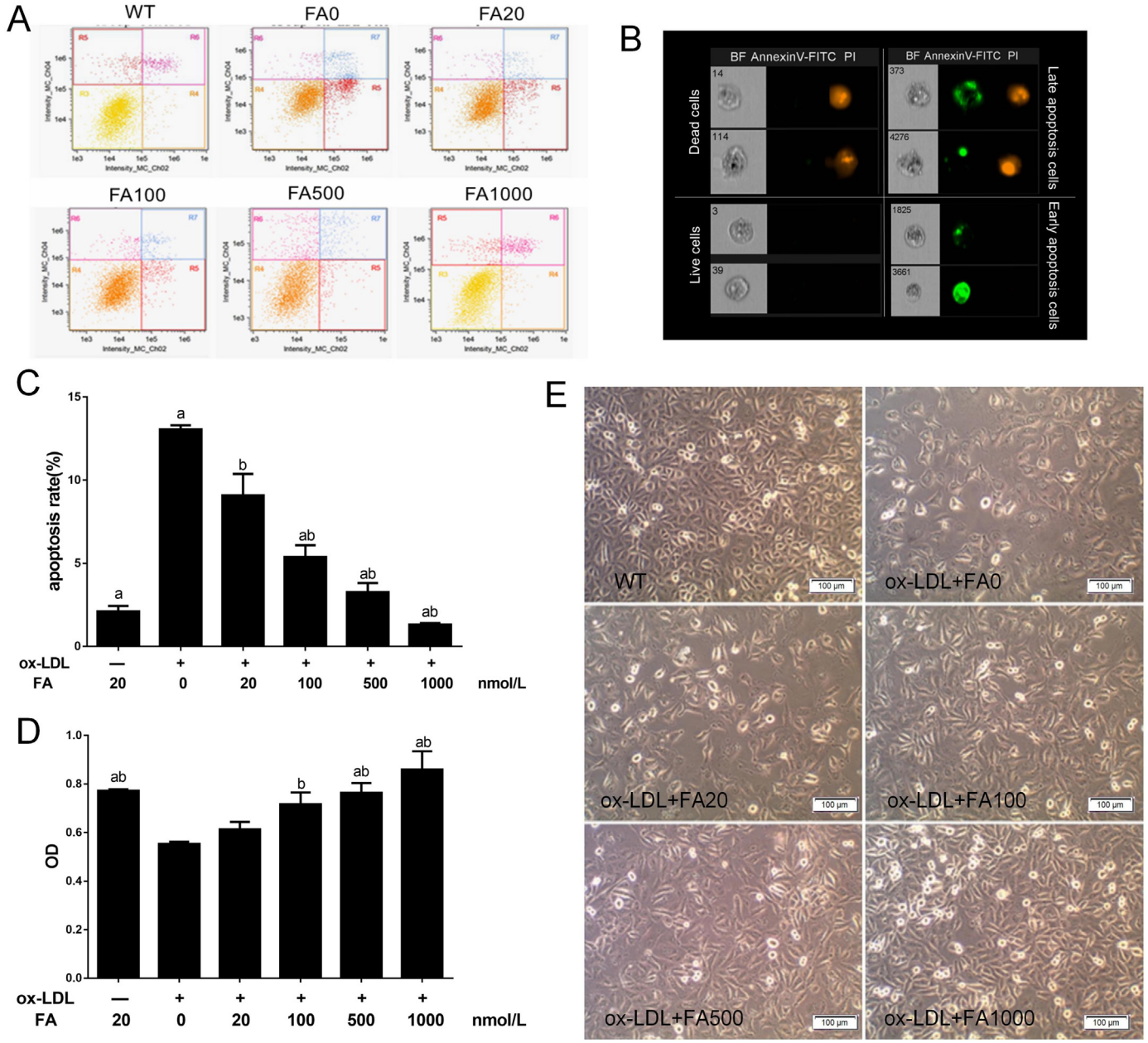

Fig. 2. Folic acid attenuated apoptosis and protected activity against ox-LDL-induced in HUVECs. HUVCE were treated with 0–1000 nmol/L folic acid for 48 h and exposed to 120 μg/mL ox-LDL for the first 24 h. (A) Apoptosis, survival and necrosis rates measured by flow cytometry with double staining of Annexin V and PI. Viable cells are shown in the lower left quadrant of each panels, which PI and Annexin V are negative (Annexin V-, PI-); the early and late apoptotic cells are shown in the lower right quadrant of each panels, which Annexin V positive and PI negative (Annexin V+, PI-); the necrotic cells are shown in the upper right quadrant of each panels, which Annexin V and PI positive (Annexin V+, PI+). (B) Representative images of unirradiated and irradiated cells obtained by the ImageStream. (C) Percentage of apoptotic by flow cytometry. (D) Cell proliferation was assayed by MTS assay. (E) The morphological change of HUVECs observed by inverted phase contrast microscope (magnification ×100). The plotted values are mean ± SE values for 3 independent experiments. a, $p < 0.05$ compared with the ox-LDL + FA20. b, $p < 0.05$ compared with the ox-LDL + FA0.

3.4. Folic acid enhances the antioxidative capacity and reduces lipid peroxidation in vitro

To determine the effect of folic acid on oxidative injuries, we measured the concentration of intracellular MDA, a marker of lipid peroxidation. We also assessed the concentration of LDH released in the medium, that of Gpx, CAT antioxidant enzymes, and SOD activity. As seen in Fig. 4, ox-LDL increased the concentration of MDA and the release of LDH and decreased CAT and SOD activities in HUVECs when compared with those in cells incubated without ox-LDL ($p < 0.05$). Furthermore, incubation with folic acid reduced the intracellular MDA concentration and the concentration of LDH released in the medium in a dose-dependent manner; this effect was significant at folic acid levels of 1000 nmol/L ($p < 0.05$ versus ox-LDL + FA20). Additionally, exposure to higher concentrations of folic acid (1000 nmol/L) significantly elevated the intracellular Gpx, CAT, and SOD activities compared with those in the Ox-LDL + FA20 group ($p < 0.05$).

3.5. Folic acid modulates ox-LDL-mediated VPO1 methylation and expression in endothelial cells

We next examined *VPO1* promoter methylation in HUVECs and

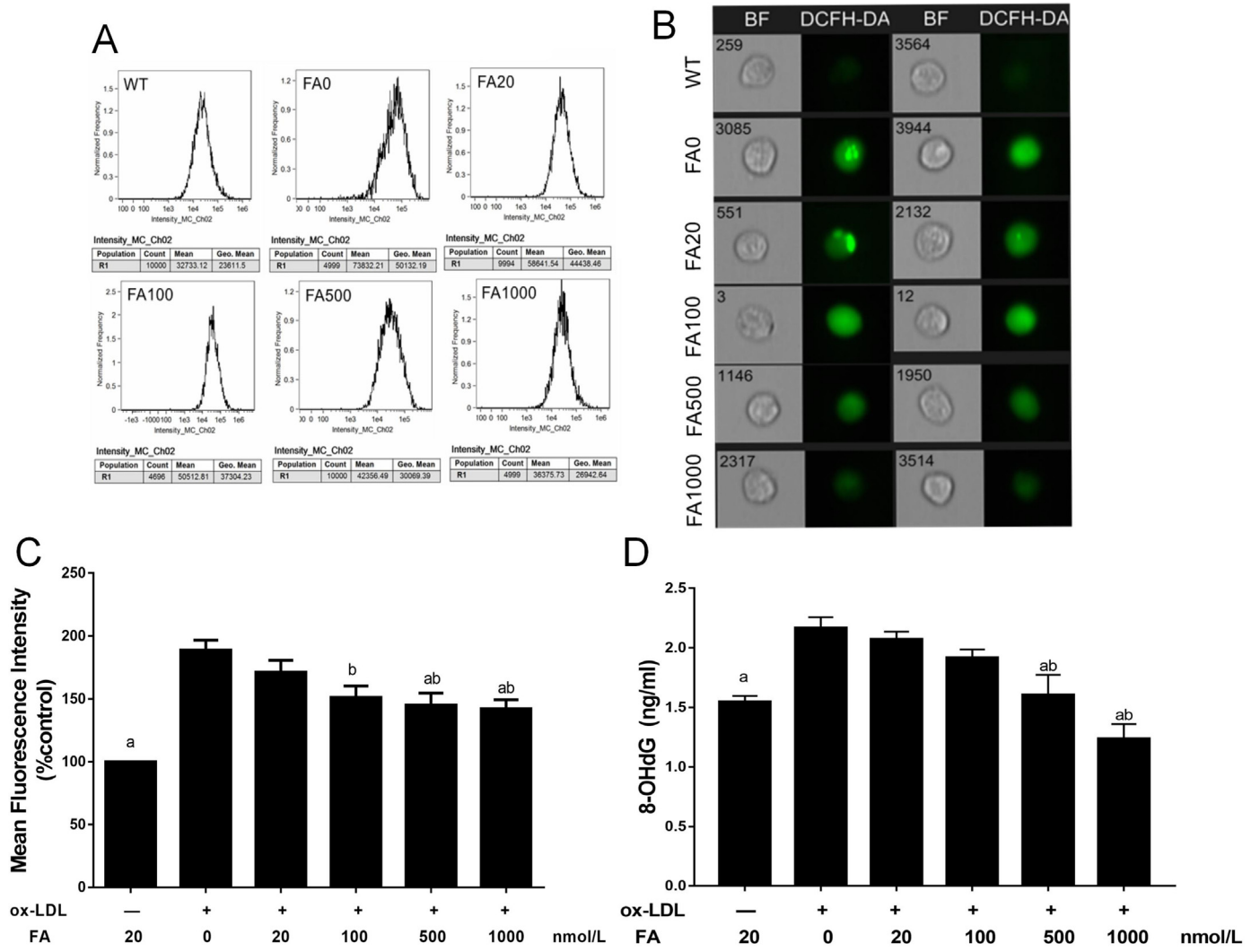

Fig. 3. The effect of folic acid on reactive oxygen species (ROS) and 8-Hydroxydeoxyguanosine (8-OHdG) level in HUVECs. HUVCE were treated with 0–1000 nmol/L folic acid for 48 h and exposed to 120 μg/mL ox-LDL for the first 24 h. (A) The intracellular ROS was measured by flow cytometry using DCFH-DA staining. The peaks in each panel represent the mean fluorescence intensities. (B) Representative images of unirradiated and irradiated cells obtained by the ImageStream. (C) ROS levels are reported as DCF Florescence, which means percentage of control group cells. (D) Intracellular 8-OHdG level was assayed by ELISA. The plotted values are mean ± SE values for 3 independent experiments. a, $p < 0.05$ compared with the ox-LDL + FA20. b, $p < 0.05$ compared with the ox-LDL + FA0.

investigated whether the expression of this gene is regulated by methylation. DNA fragments from the *VPO1* proximal promoter were divided into 26 CpG sites (Fig. 5A). Fig. 5B shows that folic acid supplementation significantly raised the methylation percentage across multiple CpG sites, as determined using a pyrosequencing assay. Specifically, methylation was significantly downregulated by folic acid deficiency at CpG sites 5, 6, and 9 in the *VPO1* promoter ($p < 0.05$ versus ox-LDL + FA20). Additionally, folic acid supplementation significantly upregulated DNA methylation at CpG sites 1, 2, 11, 14, and 15 in the *VPO1* promoter ($p < 0.05$ versus ox-LDL + FA0). Folic acid therefore modulates methylation patterns in the *VPO1* promoter in HUVECs treated with ox-LDL.

VPO1 is a newly discovered member of the peroxidase family and an important enzyme involved in the development of AS [2]. We next examined VPO1 mRNA and protein expression using real-time PCR and western blotting. Our results showed that VPO1 mRNA and protein levels were significantly increased following exposure to ox-LDL compared with those in cells cultured under normal conditions ($p < 0.05$, Fig. 5C-E). The expression of VPO1 mRNA and proteins significantly decreased by increasing the folic acid concentration (500 nmol/L) in HUVECs treated with ox-LDL ($p < 0.05$ versus that in ox-LDL + FA20).

3.6. Folic acid increases ox-LDL-induced DNMT expression and activity in endothelial cells

Our previous studies have reported changes in SAM and SAH levels in HUVECs exposed to ox-LDL [27]. It has also been shown that DNMT activity may be affected by SAM/SAH levels in cells [30]. Our results showed that DNMT activity was protected by increasing the folic acid concentration (500 nmol/L) in HUVECs treated with ox-LDL; meanwhile, a significant increase in global DNA methylation was observed in the ox-LDL + FA500 group, when compared with the ox-LDL + FA20 group ($p < 0.05$, Fig. 6A-B).

The DNMT family includes the *de novo* methyltransferase DNMT3A, DNMT3B, and the maintenance methyltransferase DNMT1. We next examined the mRNA and protein expression of DNMT1, DNMT3A, and DNMT3B using quantitative real-time PCR analysis and western blotting, respectively. Fig. 6C shows that exposure to ox-LDL decreases the mRNA expression of all DNMT isoforms compared with that in cells cultured under normal conditions ($p < 0.05$), whereas incubation with folic acid increases the mRNA expression of all DNMT isoforms; this effect was significant at folic acid levels of 1000 nmol/L ($p < 0.05$). In agreement with mRNA expression data, folic acid supplementation

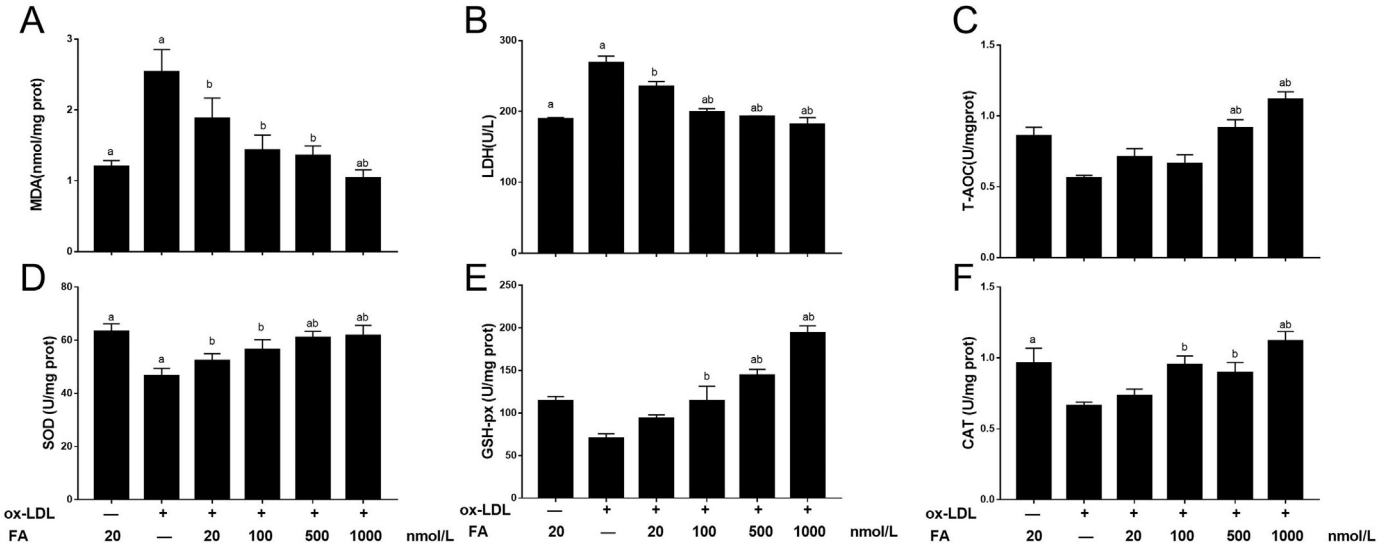

Fig. 4. Effect of folic acid on antioxidative capacity and lipid peroxidation in HUVCEs. HUVCE were treated with 0–1000 nmol/L folic acid for 48 h and exposed to 120 μg/mL ox-LDL for the first 24 h. (A) The contents of malondialdehyde (MDA) in HUVCEs. (B) The contents of lactate dehydrogenase (LDH) in the culture medium. (C) The contents of total antioxidant capability (T-AOC) in HUVCEs. (D) The activities of superoxide dismutase (SOD) in HUVCEs. (E) The activities of glutathione peroxidase (GSH-px) in HUVCEs. (F) The activities of catalase (CAT)in HUVCEs. The plotted values are mean ± SE values for 3 independent experiments. a, $p < 0.05$ compared with the ox-LDL + FA20. b, $p < 0.05$ compared with the ox-LDL + FA0.

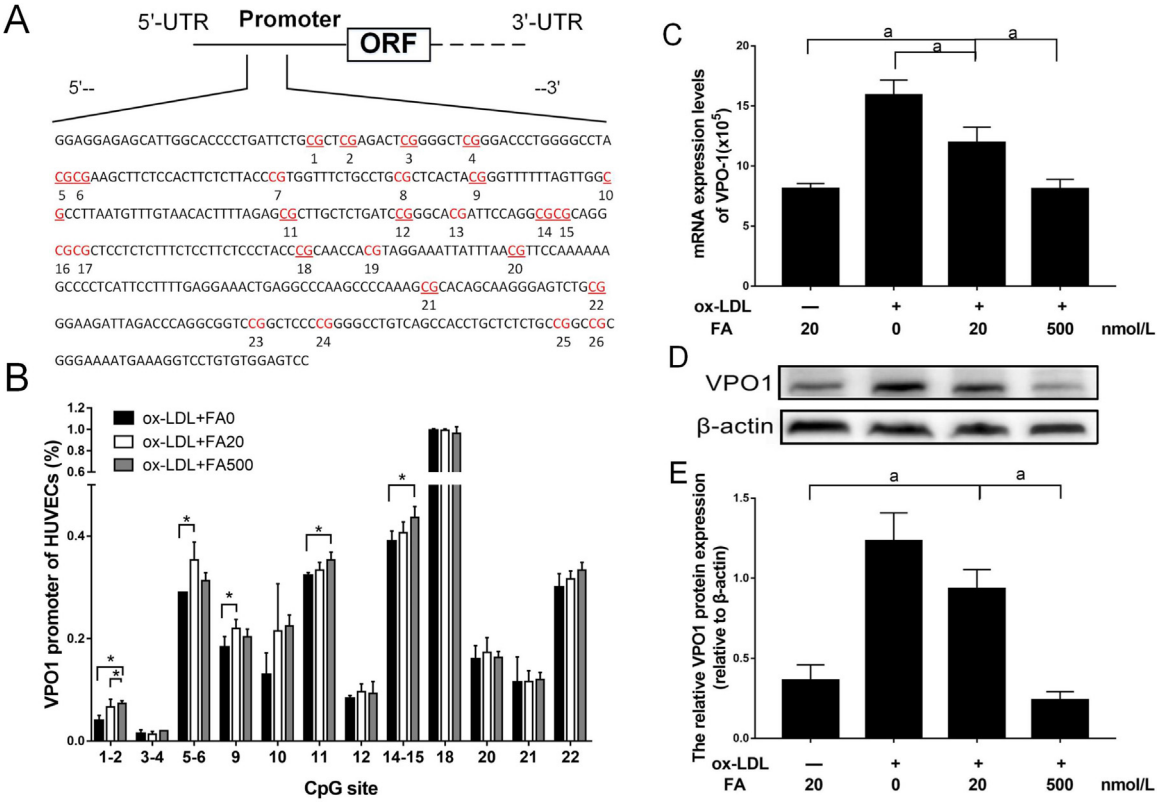

Fig. 5. Folic acid modulates the vascular peroxidase 1 (VPO1) promoter methylation levels of the CpG sites and the expression in HUVCEs. HUVCE were treated with 0–500 nmol/L folic acid for 48 h and exposed to 120 μg/mL ox-LDL for the first 24 h. (A) Schematic diagram of mice VPO1 promoter (1897–2233 bp). Pyrosequencing assay data were evaluated by dividing the VPO1 promoters into 26 CpG sites. The locations of CpG sites were indicated with red font numbers. (B) Mean methylation levels of CpG sites in VPO1 in HUVCEs. (n = 3) *, $p < 0.05$ was considered the significance of any differences between test groups. (C) Gene expression levels of VPO1 ($\times 10^3$) in HUVECs. (D) Representative western blot bands of VPO1 and β-actin proteins. (E) Semiquantitative levels of VPO1 proteins calculated by band density analysis normalized to β-actin expression. The plotted values are mean ± SE values for 3 independent experiments. a, $p < 0.05$ compared with the ox-LDL + FA20. (For interpretation of the references to color in this figure legend, the reader is referred to the web version of this article).

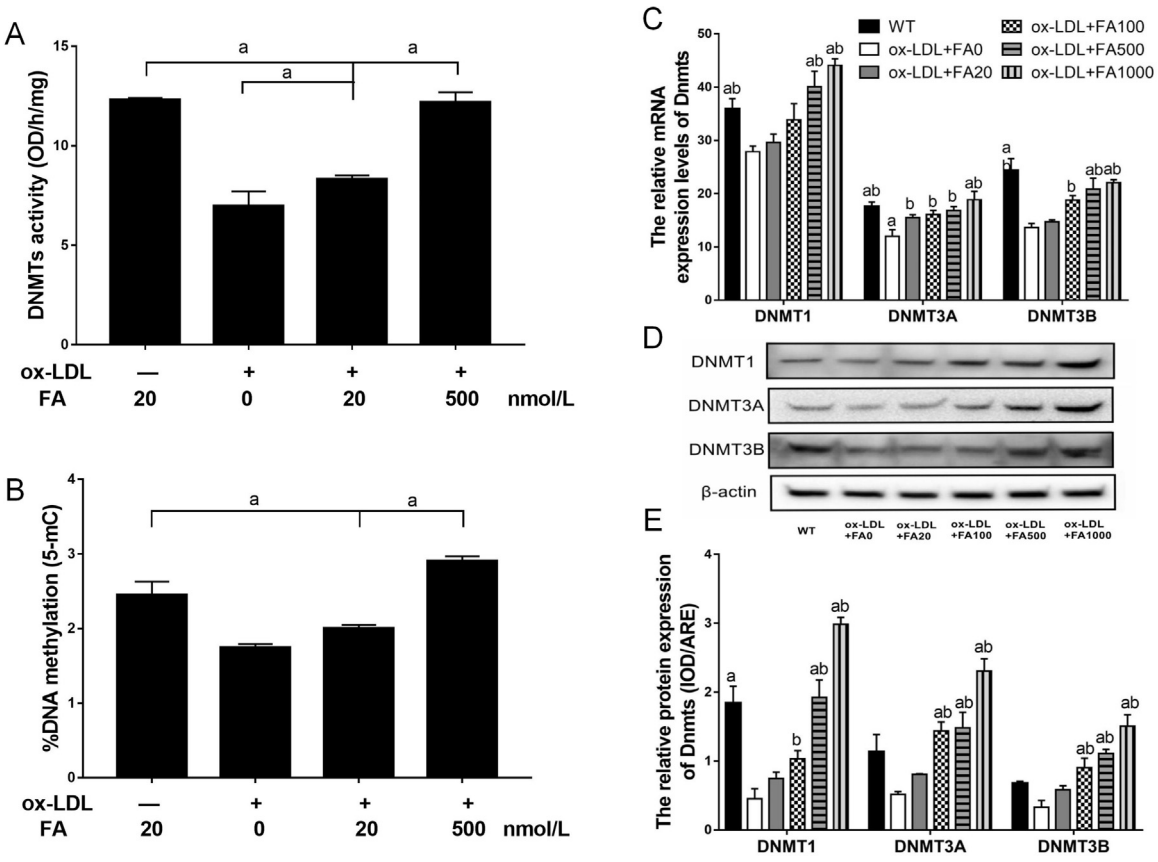

Fig. 6. Responses of DNA methyltransferase (DNMT) activity and expression in HUVCEs. HUVCE were treated with 0–1000 nmol/L folic acid for 48 h and exposed to 120 μg/mL ox-LDL for the first 24 h. (A) The total DNMTs activity in HUVECs. (B) Global methylation levels in HUVECs. The plotted values are mean ± SE values for 3 independent experiments. a, $p < 0.05$ compared with the ox-LDL + FA20. (C) Gene expression levels of DNMT1 ($\times 10^5$), DNMT3A ($\times 10^3$), and DNMT3B ($\times 10^5$) in HUVECs. (D) Representative western blot bands of DNMT1, DNMT3A, DNMT3B and β-actin proteins. (E) Semiquantitative levels of DNMT1, DNMT3A, DNMT3B proteins calculated by band density analysis normalized to β-actin expression. The plotted values are mean ± SE values for 3 independent experiments. a, $p < 0.05$ compared with the ox-LDL + FA20. b, $p < 0.05$ compared with the ox-LDL + FA0.

significantly increased the protein expression of DNMT1, DNMT3A, and DNMT3B; this effect was significant at folic acid levels of 500–1000 nmol/L ($p < 0.05$, compared with the ox-LDL + FA20 group).

4. Discussion

In the present study, we firstly demonstrated the link between folic acid supplementation and vascular endothelial dysfunction in ApoE$^{-/-}$ AS mouse models. Our data show that folic acid decreased 8-OHdG levels and reduced apoptosis in aortic tissues in ApoE$^{-/-}$ mice. The observations of our in vivo study prompted us to evaluate the mechanism underlying the protective effects of folic acid using ox-LDL-induced HUVECs in vitro. We found that folic acid protects against ox-LDL-induced endothelial dysfunction by reducing ROS-derived oxidative injuries and apoptosis. Importantly, this effect was associated with increased DNMT activity, altered DNA methylation at the *VPO1* promoter, and changes in VPO1 expression. These results indicate that oxidation-related gene methylation, oxidative stress, and their interplay may be involved in the anti-apoptotic ability of folic acid in experimental models of AS.

Today, oxidative stress remains an attractive target for CVD prevention and therapy [31]. Our results indicate that the beneficial effects of folic acid on the endothelium are mediated in part by antioxidants, underlying the ability of folic acid for the primary prevention of CVDs. Some clinical trials, such as the VISP [32], NORVIT [33], and HOPE-2 [34], have shown no benefits of B vitamin intervention for CVD prevention. However, reports from the CSPPT study [35,36] have shed new light on this controversial topic. Recent observational studies have indeed suggested that folic acid supplementation significantly improved endothelial dysfunction [21,37] and may be effective for CVD prevention [38], particularly in trials in patients without a history of grain fortification with folic acid, and healthy elderly subjects with folate deficiency. Since lower folate levels (not restricted to folate deficiency) are linked with higher rates of CVD mortality [39], folic acid as a dietary supplement is therefore required to prevent nutritional deficiency and AS in high-risk individuals. In our model, folic acid supplementation could reduce oxidative DNA damage by attenuating apoptosis in aortic tissues in ApoE$^{-/-}$ mice and ox-LDL-induced HUVECs. Collectively, we speculate that a folate supplementation strategy may lead to a protective effect on endothelial dysfunction via its anti-oxidative and anti-apoptotic effects.

The folate metabolism plays a vital role in several biological processes, including DNA, RNA, and protein methylation, as well as DNA synthesis and maintenance [40,41]. Importantly, an adequate folate status plays a critical role in the synthesis of SAM, which functions as a cofactor and methyl group donor for several methylation reactions [42]. The methylation of cytosine is catalyzed by DNMTs, where a methyl group from SAM is enzymatically transferred to generate 5-methylcytosine (5-mC) in genomic DNA [43]. Thus, an unsuitable abundance of methyl groups due to an abnormal folate metabolism results in the depletion of SAM and an overall decrease in the methylation potential (the SAM: SAH ratio) [44]. Recently, Deng et al. [45] found that global hypomethylation in blood cells, defined dominantly by monocyte DNA hypomethylation, is independently associated with the risk of coronary artery disease. Our previous studies [27] reported

that folic acid upregulated the methylation potential in vivo and in vitro. Here, we show that folic acid increases DNMT activity, the expression of functional DNMT isoforms, and the genomic 5-mC content in ox-LDL-induced HUVECs. Our results suggest that changes in folic acid abundance would disturb the DNA methylation process by altering DNMT activity.

In mammals, DNA methylation occurs at cytosine bases that are followed by a guanosine (5′-CpG-3′ sites, CpG sites) [46], and most CpG sites in DNA are methylated; CpG islands, however, remain mostly unmethylated [47]. Methylation in CpG islands, especially those islands colocalized with promoters or other regulatory regions, is typically associated with the regulation of gene expression [48,49]. This prompted us to investigate whether folic acid silences oxidation-related proteins by a similar epigenetic mechanism. This hypothesis was shown to be true, since we found that folic acid deficiency could trigger *VPO1* promoter hypomethylation, leading to increased VPO1 expression in ox-LDL-induced HUVECs. Furthermore, aberrant epigenetic regulation may contribute to the pathology of AS [50]. Our studies suggest that folic acid may inhibit oxidative damage by regulating the *VPO1* promoter methylation pattern and by silencing VPO1.

VPO1, a member of the peroxidase family found mainly in cells of the cardiovascular system [51], uses chloride and NOX-derived hydrogen peroxide (H_2O_2) to produce hypochlorous acid (HOCl), thus accelerating the development of oxidative stress in the vasculature [52,53]. In this study, ox-LDL could enhance the expression of VPO1. VPO1 may mediate the oxidation of LDL, promote the retention of LDL in vessel walls, and be a novel mediator of AS [10]. Furthermore, the results of the present study demonstrate that folic acid supplementation inhibited the further generation of ROS and the accumulation of 8-OHdG in the DNA in HUVECs, which may be mainly due to the folic acid-induced silencing of VPO1 [9]. On the other hand, in normally functioning cells, antioxidant defense systems control ROS levels; these systems consist of small antioxidant molecules and antioxidant enzymes, including SOD, Gpx, and CAT [54,55]. When cellular ROS formation exceeds the capacity of antioxidant defenses, oxidative stress occurs. Excessive production of free radicals leads to oxidative damage in lipids, proteins, and especially DNA, which may trigger an apoptotic response and atherogenic process through cellular dysfunction [56,57]. An epidemiological investigation [58] showed that low-dose folic acid therapy can improve vascular function by altering oxidative stress in vessels. We observed that higher concentrations of folic acid (1000 nmol/L) significantly elevated the intracellular Gpx, CAT, and SOD activities and reduced the intracellular MDA concentration and the concentration of LDH released in the medium. Our studies serve as a proof-of-concept, indicating that folic acid acts as an antioxidant by scavenging free radicals and enhancing the activity of antioxidant enzymes. Notably, oxidative stress can lead to DNA damage, which plays a crucial role in the development of CVD [59,60]. Moreover, several lines of evidence suggest that it might influence the induction and signaling of apoptosis in endothelial cells via different mechanisms [61–63]. In our current study, folic acid supplementation reduced the percentage of TUNEL-positive apoptotic cells in HFD ApoE$^{-/-}$ mice, promoted cell survival, and decreased apoptosis in ox-LDL-induced HUVECs. Taken together, we have identified the role of folic acid in the protection against oxidative stress damage by suppressing VPO1 via an epigenetic mechanism.

5. Conclusions

In conclusion, we demonstrate that folic acid supplementation protects against oxidative stress-induced apoptosis and suppresses ROS levels in ApoE$^{-/-}$ mice and in HUVECs exposed to ox-LDL, in which *VPO1* DNA methylation could serve as one influential factor in the process. Nevertheless, the influence of folic acid on other sources of ROS, such as nitric oxide synthase and xanthine oxidase, needs to be further investigated. These findings emphasize the importance of proper regulation of folic acid, while its deficiency can result in endothelial dysfunction. Therefore, our results offer a novel strategy to prevent AS in high-risk individuals by employing folic acid as a nutritional supplement.

Acknowledgements

This work was supported by the National Natural Science Foundation of China (Grant number 81373002).

Conflicts of interest

The authors state that they have nothing to disclose and declare no conflict of interest.

Appendix A. Supporting information

Supplementary data associated with this article can be found in the online version at doi:10.1016/j.redox.2018.08.005.

References

[1] G.B.D. Disease, I. Injury, C. Prevalence, Global, regional, and national incidence, prevalence, and years lived with disability for 328 diseases and injuries for 195 countries, 1990–2016: a systematic analysis for the global burden of disease study 2016, Lancet 390 (2017) 1211–1259.

[2] E.J. Benjamin, M.J. Blaha, S.E. Chiuve, M. Cushman, S.R. Das, R. Deo, S.D. de Ferranti, J. Floyd, M. Fornage, C. Gillespie, C.R. Isasi, M.C. Jimenez, L.C. Jordan, S.E. Judd, D. Lackland, J.H. Lichtman, L. Lisabeth, S. Liu, C.T. Longenecker, R.H. Mackey, K. Matsushita, D. Mozaffarian, M.E. Mussolino, K. Nasir, R.W. Neumar, L. Palaniappan, D.K. Pandey, R.R. Thiagarajan, M.J. Reeves, M. Ritchey, C.J. Rodriguez, G.A. Roth, W.D. Rosamond, C. Sasson, A. Towfighi, C.W. Tsao, M.B. Turner, S.S. Virani, J.H. Voeks, J.Z. Willey, J.T. Wilkins, J.H. Wu, H.M. Alger, S.S. Wong, P. Muntner, C. American Heart Association Statistics, S. Stroke Statistics, Heart disease and stroke statistics-2017 update: a report from the American heart association, Circulation 135 (2017) e146–e603.

[3] A. Schiopu, E. Bengtsson, I. Goncalves, J. Nilsson, G.N. Fredrikson, H. Bjorkbacka, Associations between macrophage colony-stimulating factor and monocyte chemotactic protein 1 in plasma and first-time coronary events: a nested case-control study, J. Am. Heart Assoc. 5 (2016).

[4] M.A. Gimbrone Jr., G. Garcia-Cardena, Endothelial cell dysfunction and the pathobiology of atherosclerosis, Circ. Res. 118 (2016) 620–636.

[5] E. Profumo, B. Buttari, D. D'Arcangelo, L. Tinaburri, M.A. Dettori, D. Fabbri, G. Delogu, R. Rigano, The nutraceutical dehydrozingerone and its dimer counteract inflammation- and oxidative stress-induced dysfunction of in vitro cultured human endothelial cells: a novel perspective for the prevention and therapy of atherosclerosis, Oxid. Med. Cell Longev. 2016 (2016) 1246485.

[6] Y. Zhang, Q. Mu, Z. Zhou, H. Song, Y. Zhang, F. Wu, M. Jiang, F. Wang, W. Zhang, L. Li, L. Shao, X. Wang, S. Li, L. Yang, Q. Wu, M. Zhang, D. Tang, Protective effect of irisin on atherosclerosis via suppressing oxidized low density lipoprotein induced vascular inflammation and endothelial dysfunction, PLoS One 11 (2016) e0158038.

[7] R. Ross, The pathogenesis of atherosclerosis: a perspective for the 1990s, Nature 362 (1993) 801–809.

[8] I. Levitan, S. Volkov, P.V. Subbaiah, Oxidized LDL: diversity, patterns of recognition, and pathophysiology, Antioxid. Redox Signal. 13 (2010) 39–75.

[9] Q.L. Ma, G.G. Zhang, J. Peng, Vascular peroxidase 1: a novel enzyme in promoting oxidative stress in cardiovascular system, Trends Cardiovasc. Med. 23 (2013) 179–183.

[10] Y. Yang, R. Shi, Z. Cao, G. Zhang, G. Cheng, VPO1 mediates oxidation of LDL and formation of foam cells, Oncotarget 7 (2016) 35500–35511.

[11] N. Khyzha, A. Alizada, M.D. Wilson, J.E. Fish, Epigenetics of atherosclerosis: emerging mechanisms and methods, Trends Mol. Med. 23 (2017) 332–347.

[12] J. Dunn, H. Qiu, S. Kim, D. Jjingo, R. Hoffman, C.W. Kim, I. Jang, D.J. Son, D. Kim, C. Pan, Y. Fan, I.K. Jordan, H. Jo, Flow-dependent epigenetic DNA methylation regulates endothelial gene expression and atherosclerosis, J. Clin. Investig. 124 (2014) 3187–3199.

[13] S. Zaina, H. Heyn, F.J. Carmona, N. Varol, S. Sayols, E. Condom, J. Ramirez-Ruz, A. Gomez, I. Goncalves, S. Moran, M. Esteller, DNA methylation map of human atherosclerosis, Circ. Cardiovasc. Genet. 7 (2014) 692–700.

[14] R. Rangel-Salazar, M. Wickstrom-Lindholm, C.A. Aguilar-Salinas, Y. Alvarado-Caudillo, K.B. Dossing, M. Esteller, E. Labourier, G. Lund, F.C. Nielsen, D. Rodriguez-Rios, M.O. Solis-Martinez, K. Wrobel, K. Wrobel, S. Zaina, Human native lipoprotein-induced de novo DNA methylation is associated with repression of inflammatory genes in THP-1 macrophages, BMC Genom. 12 (2011) 582.

[15] C. Schiano, M.T. Vietri, V. Grimaldi, A. Picascia, M.R. De Pascale, C. Napoli, Epigenetic-related therapeutic challenges in cardiovascular disease, Trends Pharmacol. Sci. 36 (2015) 226–235.

[16] R. Tirado-Magallanes, K. Rebbani, R. Lim, S. Pradhan, T. Benoukraf, Whole genome DNA methylation: beyond genes silencing, Oncotarget 8 (2017) 5629–5637.

[17] M. Okano, D.W. Bell, D.A. Haber, E. Li, DNA methyltransferases Dnmt3a and Dnmt3b are essential for de novo methylation and mammalian development, Cell 99 (1999) 247–257.
[18] R. Ostuni, V. Piccolo, I. Barozzi, S. Polletti, A. Termanini, S. Bonifacio, A. Curina, E. Prosperini, S. Ghisletti, G. Natoli, Latent enhancers activated by stimulation in differentiated cells, Cell 152 (2013) 157–171.
[19] S. Domcke, A.F. Bardet, P. Adrian Ginno, D. Hartl, L. Burger, D. Schubeler, Competition between DNA methylation and transcription factors determines binding of NRF1, Nature 528 (2015) 575–579.
[20] Dietary Reference Intakes for Thiamin, Riboflavin, Niacin, Vitamin B6, Folate, Vitamin B12, Pantothenic Acid, Biotin, and Choline. Washington (DC), 1998.
[21] L. Wang, H. Li, Y. Zhou, L. Jin, J. Liu, Low-dose B vitamins supplementation ameliorates cardiovascular risk: a double-blind randomized controlled trial in healthy Chinese elderly, Eur. J. Nutr. 54 (2015) 455–464.
[22] Y. Geng, R. Gao, X. Chen, X. Liu, X. Liao, Y. Li, S. Liu, Y. Ding, Y. Wang, J. He, Folate deficiency impairs decidualization and alters methylation patterns of the genome in mice, Mol. Hum. Reprod. 21 (2015) 844–856.
[23] Q. Yang, L.D. Botto, J.D. Erickson, R.J. Berry, C. Sambell, H. Johansen, J.M. Friedman, Improvement in stroke mortality in Canada and the United States, 1990 to 2002, Circulation 113 (2006) 1335–1343.
[24] T.G. Bentley, M.C. Weinstein, W.C. Willett, K.M. Kuntz, A cost-effectiveness analysis of folic acid fortification policy in the United States, Public Health Nutr. 12 (2009) 455–467.
[25] K.G. Lai, C.F. Chen, C.T. Ho, J.J. Liu, T.Z. Liu, C.L. Chern, Novel roles of folic acid as redox regulator: modulation of reactive oxygen species sinker protein expression and maintenance of mitochondrial redox homeostasis on hepatocellular carcinoma, Tumour Biol. 39 (2017) (1010428317702649).
[26] S. Cui, W. Li, X. Lv, P. Wang, G. Huang, Y. Gao, Folic acid attenuates homocysteine and enhances antioxidative capacity in atherosclerotic rats, Appl. Physiol. Nutr. Metab. 42 (2017) 1015–1022.
[27] S. Cui, W. Li, X. Lv, P. Wang, Y. Gao, G. Huang, Folic acid supplementation delays atherosclerotic lesion development by modulating MCP1 and VEGF DNA methylation levels in vivo and in vitro, Int J. Mol. Sci. 18 (2017).
[28] A. Lawrie, A.G. Hameed, J. Chamberlain, N. Arnold, A. Kennerley, K. Hopkinson, J. Pickworth, D.G. Kiely, D.C. Crossman, S.E. Francis, Paigen diet-fed apolipoprotein E knockout mice develop severe pulmonary hypertension in an interleukin-1-dependent manner, Am. J. Pathol. 179 (2011) 1693–1705.
[29] V. Lubrano, S. Balzan, Enzymatic antioxidant system in vascular inflammation and coronary artery disease, World J. Exp. Med. 5 (2015) 218–224.
[30] S. Jafari, M.S. Hosseini, M. Hajian, M. Forouzanfar, F. Jafarpour, P. Abedi, S. Ostadhosseini, H. Abbasi, H. Gourabi, A.H. Shahverdi, A.V. Dizaj, M. Anjomshoaa, W. Haron, N. Noorshariza, H. Yakub, M.H. Nasr-Esfahani, Improved in vitro development of cloned bovine embryos using S-adenosylhomocysteine, a non-toxic epigenetic modifying reagent, Mol. Reprod. Dev. 78 (2011) 576–584.
[31] T. Munzel, T. Gori, R.M. Bruno, S. Taddei, Is oxidative stress a therapeutic target in cardiovascular disease? Eur. Heart J. 31 (2010) 2741–2748.
[32] J.F. Toole, M.R. Malinow, L.E. Chambless, J.D. Spence, L.C. Pettigrew, V.J. Howard, E.G. Sides, C.H. Wang, M. Stampfer, Lowering homocysteine in patients with ischemic stroke to prevent recurrent stroke, myocardial infarction, and death: the vitamin intervention for stroke prevention (VISP) randomized controlled trial, JAMA 291 (2004) 565–575.
[33] K.H. Bonaa, I. Njolstad, P.M. Ueland, H. Schirmer, A. Tverdal, T. Steigen, H. Wang, J.E. Nordrehaug, E. Arnesen, K. Rasmussen, N.T. Investigators, Homocysteine lowering and cardiovascular events after acute myocardial infarction, N. Engl. J. Med. 354 (2006) 1578–1588.
[34] P. Shekelle, Lowering homocysteine with folic acid and B vitamins did not prevent vascular events in vascular disease, Evid. Based Med. 11 (2006) 104.
[35] X. Qin, J. Li, J.D. Spence, Y. Zhang, Y. Li, X. Wang, B. Wang, N. Sun, F. Chen, J. Guo, D. Yin, L. Sun, G. Tang, M. He, J. Fu, Y. Cai, X. Shi, P. Ye, H. Chen, S. Zhao, M. Chen, C. Gao, X. Kong, F.F. Hou, Y. Huang, Y. Huo, Folic acid therapy reduces the first stroke risk associated with hypercholesterolemia among hypertensive patients, Stroke 47 (2016) 2805–2812.
[36] J.D. Spence, Q. Yi, G.J. Hankey, B vitamins in stroke prevention: time to reconsider, Lancet Neurol. 16 (2017) 750–760.
[37] L.M. Title, P.M. Cummings, K. Giddens, J.J. Genest Jr., B.A. Nassar, Effect of folic acid and antioxidant vitamins on endothelial dysfunction in patients with coronary artery disease, J. Am. Coll. Cardiol. 36 (2000) 758–765.
[38] X. Qin, Y. Huo, D. Xie, F. Hou, X. Xu, X. Wang, Homocysteine-lowering therapy with folic acid is effective in cardiovascular disease prevention in patients with kidney disease: a meta-analysis of randomized controlled trials, Clin. Nutr. 32 (2013) 722–727.
[39] Y. Peng, B. Dong, Z. Wang, Serum folate concentrations and all-cause, cardiovascular disease and cancer mortality: a cohort study based on 1999–2010 national health and nutrition examination survey (NHANES), Int J. Cardiol. 219 (2016) 136–142.
[40] T.T. Yiu, W. Li, Pediatric cancer epigenome and the influence of folate, Epigenomics 7 (2015) 961–973.
[41] G.S. Ducker, J.D. Rabinowitz, One-carbon metabolism in health and disease, Cell Metab. 25 (2017) 27–42.
[42] P.R. Mandaviya, L. Stolk, S.G. Heil, Homocysteine and DNA methylation: a review of animal and human literature, Mol. Genet. Metab. 113 (2014) 243–252.
[43] S. Kundu, C.L. Peterson, Role of chromatin states in transcriptional memory, Biochim. Biophys. Acta 1790 (2009) 445–455.
[44] M.B. Glier, T.J. Green, A.M. Devlin, Methyl nutrients, DNA methylation, and cardiovascular disease, Mol. Nutr. Food Res. 58 (2014) 172–182.
[45] Q. Deng, W. Huang, C. Peng, J. Gao, Z. Li, X. Qiu, N. Yang, B. Yuan, F. Zheng, Genomic 5-mC contents in peripheral blood leukocytes were independent protective factors for coronary artery disease with a specific profile in different leukocyte subtypes, Clin. Epigenet. 10 (2018) 9.
[46] R. Holliday, G.W. Grigg, DNA methylation and mutation, Mutat. Res. 285 (1993) 61–67.
[47] A. Jeltsch, Beyond Watson and Crick: dna methylation and molecular enzymology of DNA methyltransferases, ChemBioChem 3 (2002) 274–293.
[48] D.P. Barlow, M.S. Bartolomei, Genomic imprinting in mammals, Cold Spring Harb. Perspect. Biol. 6 (2014).
[49] X. Nan, H.H. Ng, C.A. Johnson, C.D. Laherty, B.M. Turner, R.N. Eisenman, A. Bird, Transcriptional repression by the methyl-CpG-binding protein MeCP2 involves a histone deacetylase complex, Nature 393 (1998) 386–389.
[50] Z. Hai, W. Zuo, Aberrant DNA methylation in the pathogenesis of atherosclerosis, Clin. Chim. Acta 456 (2016) 69–74.
[51] G. Cheng, J.C. Salerno, Z. Cao, P.J. Pagano, J.D. Lambeth, Identification and characterization of VPO1, a new animal heme-containing peroxidase, Free Radic. Biol. Med. 45 (2008) 1682–1694.
[52] H. Li, Z. Cao, G. Zhang, V.J. Thannickal, G. Cheng, Vascular peroxidase 1 catalyzes the formation of hypohalous acids: characterization of its substrate specificity and enzymatic properties, Free Radic. Biol. Med. 53 (2012) 1954–1959.
[53] H. Li, Z. Cao, D.R. Moore, P.L. Jackson, S. Barnes, J.D. Lambeth, V.J. Thannickal, G. Cheng, Microbicidal activity of vascular peroxidase 1 in human plasma via generation of hypochlorous acid, Infect. Immun. 80 (2012) 2528–2537.
[54] A. Formigari, P. Irato, A. Santon, Zinc, antioxidant systems and metallothionein in metal mediated-apoptosis: biochemical and cytochemical aspects, Comp. Biochem. Physiol. C Toxicol. Pharmacol. 146 (2007) 443–459.
[55] N. Tadepalle, Y. Koehler, M. Brandmann, N. Meyer, R. Dringen, Arsenite stimulates glutathione export and glycolytic flux in viable primary rat brain astrocytes, Neurochem. Int. 76 (2014) 1–11.
[56] T.V. Bagnyukova, C.L. Powell, O. Pavliv, V.P. Tryndyak, I.P. Pogribny, Induction of oxidative stress and DNA damage in rat brain by a folate/methyl-deficient diet, Brain Res. 1237 (2008) 44–51.
[57] J. Stark, Oxidative stress and atherosclerosis, Orv. Hetil. 156 (2015) 1115–1119.
[58] C. Shirodaria, C. Antoniades, J. Lee, C.E. Jackson, M.D. Robson, J.M. Francis, S.J. Moat, C. Ratnatunga, R. Pillai, H. Refsum, S. Neubauer, K.M. Channon, Global improvement of vascular function and redox state with low-dose folic acid: implications for folate therapy in patients with coronary artery disease, Circulation 115 (2007) 2262–2270.
[59] J. Marin-Garcia, Mitochondrial DNA repair: a novel therapeutic target for heart failure, Heart Fail Rev. 21 (2016) 475–487.
[60] N.K. Mondal, E. Sorensen, N. Hiivala, E. Feller, B. Griffith, Z.J. Wu, Oxidative stress, DNA damage and repair in heart failure patients after implantation of continuous flow left ventricular assist devices, Int. J. Med. Sci. 10 (2013) 883–893.
[61] J. Loscalzo, Oxidant stress: a key determinant of atherothrombosis, Biochem. Soc. Trans. 31 (2003) 1059–1061.
[62] U. Landmesser, D.G. Harrison, Oxidant stress as a marker for cardiovascular events: Ox marks the spot, Circulation 104 (2001) 2638–2640.
[63] K. Korybalska, E. Kawka, A. Kusch, F. Aregger, D. Dragun, A. Jorres, A. Breborowicz, J. Witowski, Recovery of senescent endothelial cells from injury, J. Gerontol. A Biol. Sci. Med. Sci. 68 (2013) 250–257.